The piRNA-pathway factor FKBP6 is essential for spermatogenesis but dispensable for control of meiotic LINE-1 expression in humans

Graphical abstract

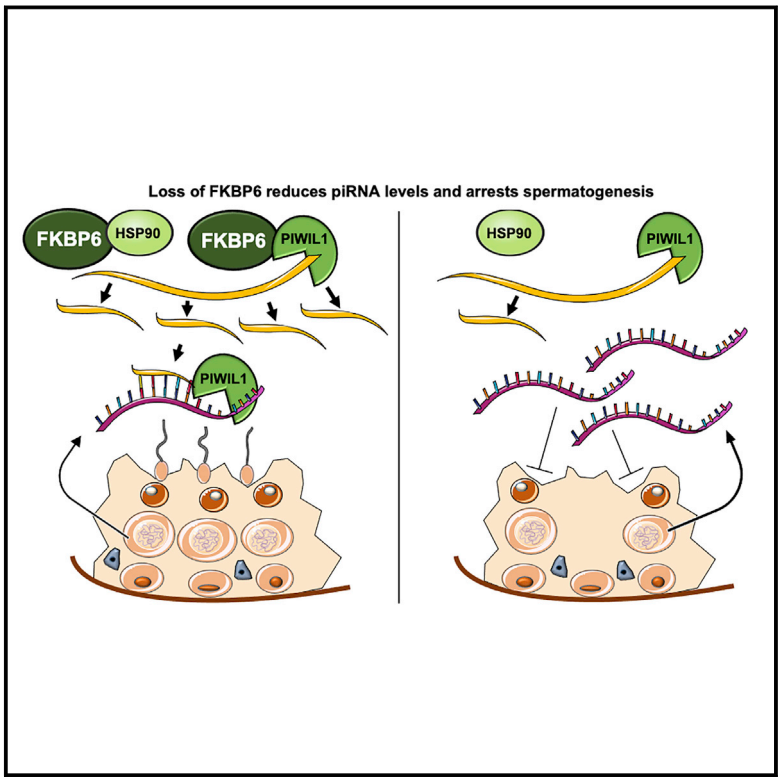

Authors

Margot J. Wyrwoll,
Channah M. Gaasbeek,
Ieva Golubickaite, ..., Joris A. Veltman,
Frank Tüttelmann,
Godfried W. van der Heijden

Correspondence

godfried.vanderheijden@radboudumc.nl

Bi-allelic loss-of-function variants in *FKBP6* cause human male infertility due to round spermatid arrest. Absence of this piRNA factor leads to a reduction of pachytene piRNAs, which likely disrupts piRNA-mediated translational regulation in germ cells from mid-meiosis on. In contrast to many piRNA-factor mouse models, LINE-1 overexpression is not observed.

Wyrwoll et al., 2022, The American Journal of Human Genetics *109*, 1850–1866
October 6, 2022
https://doi.org/10.1016/j.ajhg.2022.09.002

CellPress

ARTICLE

The piRNA-pathway factor FKBP6 is essential for spermatogenesis but dispensable for control of meiotic LINE-1 expression in humans

Margot J. Wyrwoll,[1,23] Channah M. Gaasbeek,[2,3,4,23] Ieva Golubickaite,[5,6,7] Rytis Stakaitis,[5,6,8] Manon S. Oud,[2,3] Liina Nagirnaja,[5] Camille Dion,[9,10] Emad B. Sindi,[11] Harry G. Leitch,[9,10,12] Channa N. Jayasena,[11] Anu Sironen,[13,14] Ann-Kristin Dicke,[1] Nadja Rotte,[1] Birgit Stallmeyer,[1] Sabine Kliesch,[15] Carlos H.P. Grangeiro,[16] Thaís F. Araujo,[17] Paul Lasko,[2,18] Genetics of Male Infertility Initiative (GEMINI) consortium, Kathleen D'Hauwers,[19] Roos M. Smits,[4] Liliana Ramos,[4] Miguel J. Xavier,[20] Don F. Conrad,[5] Kristian Almstrup,[21,22] Joris A. Veltman,[20] Frank Tüttelmann,[1] and Godfried W. van der Heijden[4,*]

Summary

Infertility affects around 7% of the male population and can be due to severe spermatogenic failure (SPGF), resulting in no or very few sperm in the ejaculate. We initially identified a homozygous frameshift variant in *FKBP6* in a man with extreme oligozoospermia. Subsequently, we screened a total of 2,699 men with SPGF and detected rare bi-allelic loss-of-function variants in *FKBP6* in five additional persons. All six individuals had no or extremely few sperm in the ejaculate, which were not suitable for medically assisted reproduction. Evaluation of testicular tissue revealed an arrest at the stage of round spermatids. Lack of FKBP6 expression in the testis was confirmed by RT-qPCR and immunofluorescence staining. In mice, Fkbp6 is essential for spermatogenesis and has been described as being involved in piRNA biogenesis and formation of the synaptonemal complex (SC). We did not detect FKBP6 as part of the SC in normal human spermatocytes, but small RNA sequencing revealed that loss of FKBP6 severely impacted piRNA levels, supporting a role for FKBP6 in piRNA biogenesis in humans. In contrast to findings in piRNA-pathway mouse models, we did not detect an increase in LINE-1 expression in men with pathogenic *FKBP6* variants. Based on our findings, *FKBP6* reaches a "strong" level of evidence for being associated with male infertility according to the ClinGen criteria, making it directly applicable for clinical diagnostics. This will improve patient care by providing a causal diagnosis and will help to predict chances for successful surgical sperm retrieval.

Introduction

Male infertility, which affects around 7% of all men, is in half of all cases due to decreased sperm counts,[1] called oligozoospermia. Extreme oligozoospermia, of which cryptozoospermia is a subform, is defined as the most severe form of oligozoospermia with less than 100,000 sperm cells present per mL of ejaculate.[2] This condition forms a continuum with azoospermia, in which the ejaculate lacks sperm completely. Both can be observed in the same individual in repeated semen analyses. The two conditions are commonly due to severe spermatogenic failure (SPGF).[3] Sperm detected in the ejaculate of men with SPGF are not always suitable for medically assisted reproduction (MAR), as they may be necrotic or may have major morphological abnormalities. In this case a testicular biopsy with the aim of testicular sperm extraction (TESE) is offered to the man. SPGF can be due to arrests at specific stages of spermatogenesis, e.g., during meiosis (meiotic arrest; MeiA) or downstream of meiosis during spermiogenesis, resulting in round spermatid arrest (RsA).[4] Under these circumstances, TESE is unlikely to be successful and the chance to father a child is diminutive.

After andrological work-up, the majority of persons with SPGF remain without a causal diagnosis.[1] While not extensively evaluated diagnostically in most persons, genetics

[1]Institute of Reproductive Genetics, University of Münster, Münster, Germany; [2]Department of Human Genetics, Radboudumc, Nijmegen, the Netherlands; [3]Donders Institute for Brain, Cognition and Behaviour, Radboudumc, Nijmegen, the Netherlands; [4]Department of Obstetrics and Gynecology, Radboud University Medical Center, Nijmegen, the Netherlands; [5]Division of Genetics, Oregon National Primate Research Center, Oregon Health and Science University, Beaverton, OR, USA; [6]Department of Growth and Reproduction, Copenhagen University Hospital – Rigshospitalet, Copenhagen, Denmark; [7]Department of Genetics and Molecular Medicine, Lithuanian University of Health Sciences, Kaunas, Lithuania; [8]Laboratory of Molecular Neurooncology, Neuroscience Institute, Lithuanian University of Health Sciences, Kaunas, Lithuania; [9]MRC London Institute of Medical Sciences, London, UK; [10]Institute of Clinical Sciences, Imperial College London, London, UK; [11]Section of Investigative Medicine, Imperial College London, London, UK; [12]Centre for Paediatrics and Child Health, Faculty of Medicine, Imperial College London, London, UK; [13]Natural Resources Institute Finland, Production Systems, Jokioinen, Finland; [14]Great Ormond Street Institute of Child Health, University College London, London, UK; [15]Centre of Reproductive Medicine and Andrology, Department of Clinical and Surgical Andrology, University Hospital of Münster, Münster, Germany; [16]Complexo Hospitalar of Federal University of Ceará, Fortaleza, Brazil; [17]Department of Genetics, Ribeirão Preto Medical School, University of São Paulo, Ribeirão Preto, Brazil; [18]Department of Biology, McGill University, Montréal, QC, Canada; [19]Department of Urology, Radboudumc, Nijmegen, the Netherlands; [20]Biosciences Institute, Faculty of Medical Sciences, Newcastle University, Newcastle Upon Tyne, UK; [21]Department of Growth and Reproduction, Copenhagen University Hospital – Rigshospitalet, Copenhagen, Denmark; [22]Department of Cellular and Molecular Medicine, Faculty of Health and Medical Sciences, University of Copenhagen, Copenhagen, Denmark
[23]These authors contributed equally
*Correspondence: godfried.vanderheijden@radboudumc.nl
https://doi.org/10.1016/j.ajhg.2022.09.002.

are known to play a major role in SPGF.[5] Various genes have been described to be associated with impaired spermatogenesis. Of interest for this work specifically are bi-allelic variants in the piRNA gene *PNLDC1* which were recently described in four azoospermic men, suggesting a direct mechanistic effect of faulty piRNA processing during spermatogenesis in men.[6] The piRNA pathway consists of PIWI (P element induced wimpy testis)-interacting RNAs (piRNAs), PIWI proteins (PIWIL1, PIWIL2, PIWIL3 and PIWIL4), and accessory proteins. The piRNAs lend sequence specificity to the RNA-processing PIWI proteins. Complexed with a piRNA as a guide, PIWI proteins can degrade specific transcripts and delay or induce mRNA translation (PIWIL1 and PIWIL2) or direct DNA methylation (PIWIL3 and PIWIL4).[7–10] The two canonical functions of the pathway are the control of transposable elements (TEs) in both the fetal and adult testis[11–14] and the translational regulation of protein coding genes in the adult testis.[8,15–17]

piRNAs derive from long non-coding RNAs transcribed from genomic piRNA clusters that are processed into piRNAs (primary biogenesis) or can be derived from untranslated regions of mRNAs in a ping-pong amplification to enhance their numbers (secondary processing).[7,18] Whereas both primary and secondary processing contribute to the piRNA pool in fetal male germ cells, in adult male germ cells piRNAs are primarily generated via primary biogenesis.[19]

In the adult testis, three classes of piRNAs, which differ in their expression pattern and sequence content, have been identified: pre-pachytene, pachytene, and hybrid. The pre-pachytene piRNAs are directed more towards TE control whereas the pachytene piRNAs are more involved in regulating post-meiotic gene expression.[7,15–17] Knockout (KO) mouse models for genes encoding proteins involved in the piRNA biogenesis have shown that virtually all of these proteins are essential for spermatogenesis in mice as most of these mice models exhibit male specific infertility due to MeiA or RsA.[7,18,20] In humans, bi-allelic variants in the piRNA biogenesis-related genes *TDRD7*, *TDRD9, PNLDC1*, and *MOV10L1* have been identified in infertile men with (partial) MeiA so far.[6,21–23]

Another gene, FKBP Prolyl Isomerase Family Member 6 (*Fkbp6* [MIM: 604839]), has been linked to the secondary piRNA biogenesis in fetal male mouse germ cells.[24] In male rodents and *Drosophila*, inactivation of *Fkbp6* or its ortholog results in a severe reduction of piRNA production, leading to an increased expression of TEs and infertility.[24,25] Fkbp6 belongs to the FK506 Binding Protein family, characterized by an FKBP domain which has a peptidyl-propyl *cis-trans* isomerase activity.[26] In FKBP6, this domain has lost this ability.[24] Downstream is a tetratricopeptide repeat (TPR) domain, which facilitates protein-protein interactions, especially with heat shock proteins.[24,27] In accordance, in mice, Fkbp6 has been shown to bind the heat shock protein Hsp90, which is involved in the piRNA pathway.[28] Furthermore, Fkbp6 also directly interacts with central piRNA components Miwi (Piwil1), Miwi2 (Piwil4), and Tdrd1, which are known to be essential for piRNA biogenesis.[24,29,30] Prior to the discovery of the piRNA pathway, murine Fkbp6 was identified as a component of the synaptonemal complex (SC).[31] In male mice, loss of Fkbp6 results in impaired meiosis and subsequent azoospermia, presumably due to incomplete chromosomal synapsis, whereas female mice are fertile.[31] Still, it remains unclear whether the observed impairment of chromosomal synapsis in male mice occurs in the context of impaired piRNA biogenesis.

Here, we present data that introduces *FKBP6* as an essential gene for human spermatogenesis. We describe six unrelated individuals in which bi-allelic pathogenic variants in *FKBP6* are the most likely causal explanation for their observed SPGF.

Subjects and methods

Exome sequencing in RU02135 and his parents

RU02135 and his wife attended the fertility center at Radboudumc because of the couple's infertility. Semen analysis revealed extreme oligozoospermia, whereas no reason for infertility was found in his wife. Exome sequencing for scientific purposes was performed on DNA from RU02135 and his parents. Exome library preparation was performed using Twist Human Core Exome Kit and dual-indexed with the Twist Universal Adapters (Twist Biosciences). Sequencing was performed using the NovaSeq 6000 platform, Genomics Core Facility of the Faculty of Medical Sciences at Newcastle University, UK. Read mapping and SNV and CNV calling were performed as described earlier.[32] Homozygosity calling was performed using RareVariantVis.[33]

Filtering strategy in RU02135 and his parents

The exome sequencing data were filtered for non-synonymous coding variants or splice site variants that were present in >5 variant sequencing reads and were present in >15% of reads covering that locus. A minor allele frequency (MAF) of <0.01 was used for autosomal variants, for gonosomal variants we used <0.001 according to gnomAD,[34] NCBI dbSNP and to our in-house database (containing >15,000 alleles). Data were screened for genes with compound heterozygous variants or homozygous variants that were present heterozygous in both parents, genes with *de novo* mutations, and genes with maternally inherited X-linked variants. The quality of all prioritized variants was manually curated in the Integrative Genomics Viewer 2.4[35] and classified according to the ACMG-AMP guidelines.[36] Prioritized variants (Table S1) were validated by Sanger sequencing. As a control cohort, we used exome-sequencing data of 11,587 fertile parents (5,784 fathers and 5,803 mothers) sequenced at the Radboudumc Genome Diagnostics Centre in Nijmegen, the Netherlands, as previously described.[37]

Exome sequencing in the MERGE, Imperial, and GEMINI cohort

Three additional cohorts of infertile men were investigated to identify affected individuals with bi-allelic variants in *FKBP6*. The MERGE cohort comprises 1,671 men with various infertility phenotypes as well as small group of fertile control men. Most

men of this cohort are azoospermic (n = 1,043) or severe oligozoospermic (n = 386). Exome sequencing and bioinformatics analysis in the MERGE cohort were performed as previously described.[38]

The GEMINI cohort comprises 1,011 men diagnosed with spermatogenic failure. The vast majority of these men has unexplained NOA, while genetic causes have been identified in some of them.[6,32,37,39–42] Exome sequencing in the GEMINI cohort was performed as previously described.[32]

The Imperial cohort comprises 17 infertile men who are all azoospermic. Exome sequencing in the Imperial cohort was performed as described in the supplemental methods.

We screened the exome-sequencing data of the MERGE, GEMINI, and Imperial cohort for stop-gain, splice site, and missense variants in *FKBP6*, with a MAF <0.01 according to the gnomAD database (v.2.1.1).

Sanger sequencing validation was performed for all *FKBP6* variants according to local standard procedures. If DNA from family members was available for segregation analysis, this was done by Sanger sequencing. The respective primer sequences can be found in the supplemental methods. Relatedness between RU02135, M2546, and M2548 was estimated using the Somalier tool.[43] The effect of splice site variants was investigated with the minigene assay (supplemental information).

Variant and gene assessment

The *FKBP6* variants were assessed according to the ACMG-AMP criteria,[36] adapted by the recommendations of the ClinGen Sequence Variant Interpretation Working Group.[44,45] Based on the literature and our data, we assessed the clinical validity of *FKBP6* in the context of male infertility according to the criteria established by the ClinGen working group.[46]

Ethical approval

All persons gave written consent compliant with local requirements. Exome sequencing in RU02135 was approved by the Radboud UMC Institutional Review Board (Ref. No. NL50495.091.14 version 5). The MERGE study protocol was approved by the Münster Ethics Committees/Institutional Review Boards (Ref. No. Münster: 2010-578-f-S) in accordance with the Helsinki Declaration of 1975. The study protocol of the GEMINI cohort was approved by the Ethics Committee of all its collaborative centers: IRB protocols #201107177 and #201109261 for Washington University in St. Louis, USA; IRB_00063950 for University of Utah, USA; PTDC/SAU-GMG/101229/2008 for Porto, Portugal; and approvals from human ethics committees of Monash Surgical Day Hospital, Monash Medical Centre and Monash University, Australia. The study protocol of the Imperial cohort was approved by the West London & GTAC Research Ethics Committee (Ref. No. 14/LO/1038).

FKBP6 transcript isoforms and FKBP6 antibody

According to GTEx *FKBP6* encodes seven hypothetical transcript isoforms of which four are expressed as protein: (1) ENST00000252037.5, (2) ENST00000431982.6, (3) ENST00000442793.5, and (4) ENST00000413573.6. Transcript 1 is the canonical one and differs from transcript 2 and 3 in the first exon whereas transcript 4 lacks the third exon. The transcript per kilobase million (TPM) for these four transcripts are respectively 38.31, 19.44, 16.73, and 4.22 (GTEx). The commercial antibody against FKBP6 used in this study is a mouse monoclonal antibody raised against a peptide spanning amino acid (aa) 1–108 of transcript 1. The precise location of the epitope is unknown. The first 19 aa of this peptide, representing exon 1, are not shared with transcript 2 and 3 but the remaining 89 aa are.

Meiotic analyses

The meiotic status of spermatocytes was determined by (1) DAPI staining, (2) antibody staining against γH2AX, and (3) location of the cell in the seminiferous epithelium. To ensure that only meiotic prophase I (MPI) cells were counted in the quantification of apoptotic cells, we excluded apoptotic cells close to the basal lamina (likely spermatogonia); apoptotic cells with condensed chromosomes (likely meiotic metaphases); and apoptotic cells with a smaller nucleus, closer to the lumen (likely spermatids). To detect meiotic metaphases, an antibody against histone H3S10ph, a marker of "mitotic" chromatin, was used. Only H3S10ph-positive cells closer to the lumen of the seminiferous tubules were taken into account. Further information is available in the supplemental methods.

RNA extraction

RNA from FFPE samples of RU02135, of the controls C13-1336 and C12-841, and of RU02092, who is affected by a homozygous *PNLDC1* variant (GenBank: NM_173516.2; c.607−2A>T), was extracted using Recover All Total Nucleic Acid Isolation Kit for FFPE (Invitrogen, Cat. #AM1975). RNA from snap-frozen testicular tissues of the controls SSC764, M2350, and M2676 and individuals M1400, M2546, and M2548 was extracted using Direct-zol RNA Microprep kit (Zymo Research, Cat. #R2062).

The quantity and quality of the isolated RNA were assessed with Qubit RNA High Sensitivity kit (Inivitrogen, Cat. #Q32852) and Agilent RNA Nano kit (Agilent, Cat. #55067-1512), respectively.

Real time-qPCR

cDNA was synthesized by reverse transcription of RNA using AffinityScript qPCR cDNA Synthesis Kit (Agilent, Cat. #600559) or Superscript IV First-Strand Synthesis System Kit (Invitrogen, Cat. #18091050). Real time (RT)-qPCR was performed on QuantStudio 3 (Applied Biosystems, Cat. #A28137), using PowerUp SYBR Green Master Mix (Applied biosystems, Cat. # A25741) and 0.15 μM of gene-specific primers (Integrated DNA Technologies). The RT-qPCR reaction included initial denaturation (2 min at 50°C and 2 min at 95°C) and amplification (45 cycles of 15 s at 95°C followed by 60 s at 62°C) steps. A melting curve procedure was performed at the end of every RT-qPCR run to check for unspecific PCR products. Primers are listed in the supplemental methods.

Small RNA sequencing

100 ng of total RNA from samples C13-1336, C12-841, RU02135, SSC764, and M1400 was used to build small RNA libraries applying CATS small RNA-seq kit (Diagenode, Cat. #C05010040). Small RNAs were sequenced according to previously published protocols.[6] In addition to the manufacturer's protocol, a spike-in mix (Qiagen, Cat. # 331535) was added at the initial library preparation step, to check for technical errors at library preparation and sequencing steps. 1.5 nM of each library was used for sequencing preparation following Illumina protocol (Illumina, Doc. # 15039740 v10, Protocol A: Standard normalization). In total, two 1 × 50 cycle sequencing runs were performed on Illumina MiSeq using MiSeq Reagent Kit v2 (Illumina, Cat. # SY-410-1003; and # MS-102-2001). On each run, two samples were sequenced, with the affected man and the control on the same flow cell. On average, 130k reads were generated for each sample.

300 ng of total RNA from samples M2350, M2676, M2546, and M2548 was used for small RNA library preparation using NEXTflex Small RNA-Seq Kit v3 (PerkinElmer, Cat. #NOVA-5132-05). In addition to the manufacturer's protocol, a spike-in mix of 0.05 ng 5′P-cel-miR-39-3p-3′-OH and 0.05 ng 5′P-ath-159a-3′-2-OMe was added at the initial library preparation step, to check for technical errors at library preparation and sequencing steps. Sequencing was carried out at the OHSU Massively Parallel Sequencing Shared Resource facilities on Illumina NovaSeq 6000 S4 2x100 flow cell. All four samples were sequenced on the same lane of the flow cell.

RNA-seq data processing and piRNA annotation

First, sequencing reads were trimmed with Cutadapt (v.#3.0)[47] according to instructions provided by CATS small RNAseq kit protocol (Diagenode, Cat. #C05010040, Doc. # v.2 I 09.17) or NEXTflex Small RNA-Seq Kit protocol (PerkinElmer, Cat. #NOVA-5132-05, Doc. # v.V19.01). Next, trimmed reads were aligned to reference genome (GRCh37) with Bowtie (v.#1.0.1)[48] allowing only perfect matches, discarded miRNAs by selecting reads between 25 and 45 bases, and re-aligned to GRCh37 allowing one mismatch. Finally, known small non-coding RNAs, other than piRNAs, were removed from the dataset using DASHRv2 (v.#v2),[49] and the remaining piRNA sequences were intersected with known piRNA loci detected in human adult testis.[50]

Statistical analysis

The testicular cells quantified in affected persons and control subjects were compared and statistically analyzed using a chi-squared test to detect differences between groups. All statistical analyses were performed using R statistical software.[51] Data from RT-qPCR and small RNA-seq experiments were evaluated using SciPy (ver.: 1.8.0) packages[52]: Shapiro-Wilk test for normality of the data and Student's T-test for expression changes in RT-qPCR and for changes in piRNA quantities of different lengths were used.

Results

Trio-based exome sequencing revealed a homozygous frameshift variant in *FKBP6*

25,098 sequence variants were obtained by exome sequencing in the index subject RU02135. Of these, 624 variants were predicted to alter the coding protein sequence (missense, splice site, frameshift, stop-gain variants) and were classified as rare according to their global frequency in the gnomAD database (MAF <0.01 for autosomal, <0.001 for gonosomal variants). Exome sequencing of both parents allowed for further narrowing down of candidate variants by focusing on confirmed compound heterozygous (n = 43) and homozygous (n = 5) variants inherited from both parents, maternally inherited X-linked variants (n = 3), and *de novo* variants (n = 6). Variants that were found to be a sequencing artifact or calling error upon manual inspection of the data, failure to validate using Sanger sequencing, and/or variants with a (likely) benign classification according to the ACMG-AMP criteria were discarded from further analysis, leaving a total of six genes affected with possibly pathogenic variants: *FKBP6* with a homozygous loss-of-function (LoF) variant; *B3GNT8*, *EEF2K*, and *TTN* with compound heterozygous missense variants; and *CACNA1F* and *L1CAM* with hemizygous missense variants. Of these, the homozygous LoF variant in *FKBP6* was prioritized based on the high and unique expression of *FKBP6* in the testis, its essential role in mouse spermatogenesis,[31] and the predicted impact on protein function (Table S1; Figure S1).

The homozygous duplication of 22 base pairs (bp) within exon 5 of *FKBP6* (GenBank: NM_003602.4: c.508_529dup) leading to a frameshift within the open reading frame (p.Phe177CysfsTer20) (Figures 1A and 1J) was observed in the affected men. Both unaffected parents were confirmed to carry this variant heterozygous (Figure S2). This variant is listed in gnomAD with a frequency of 0.019%, with no homozygous individuals reported. In a Dutch control cohort of 5,784 fathers and 5,803 mothers originating from the same region as the index case subject, we observed a total of 18 heterozygous carriers of the identical variant in *FKBP6* (8 fathers, 10 mothers). This indicates a higher MAF of 0.078% for this variant in the Dutch proven parent population compared to gnomAD database. None of these fathers or mothers was homozygous for this variant or was identified with any other rare variant in *FKBP6*.

Five additional men with (likely) pathogenic *FKBP6* variants

To determine whether bi-allelic *FKPB6* variants are a recurrent cause of male infertility, we screened a total of 2,699 infertile men (1,671 men from the MERGE cohort, 1,011 men from the GEMINI cohort, and 17 individuals from the Imperial cohort) for further variants. In the GEMINI cohort, no individuals with rare bi-allelic variants in *FKBP6* were identified. Within the MERGE cohort, we identified four men with bi-allelic LoF variants in *FKBP6* and an additional individual with a homozygous LoF variant was found in the Imperial cohort (Table 1; supplemental information). Individual M2548 was identified with the same homozygous 22 base pairs (bp) insertion as identified in RU21035, resulting in a frameshift to the coding sequence c.508_529dup (p.Phe177CysfsTer20) (Figures 1F and 1J). Individual M2546 was found to with the same frameshift variant c.508_529dup (p.Phe177CysfsTer20) but in a heterozygous state in combination with a heterozygous stop-gain variant c.832C>T (p.Arg278Ter) in *FKBP6* in the opposite allele (Figures 1D, 1E, and 1J). Compound heterozygosity was confirmed after the mother was found to be a heterozygous carrier of the c.832C>T (p.Arg278Ter) variant, and the other variant was not present in her genome. Unfortunately, the DNA from the father was not available, but the proband has three sisters of which DNA was available for two of them. All three sisters have at least two children and premature ovarian insufficiency (POI) was not reported for any of the sisters. The youngest sister carries none of the *FKBP6* variants, whereas the older sister was compound heterozygous for both *FKBP6* variants (Figure 1H), making it extremely

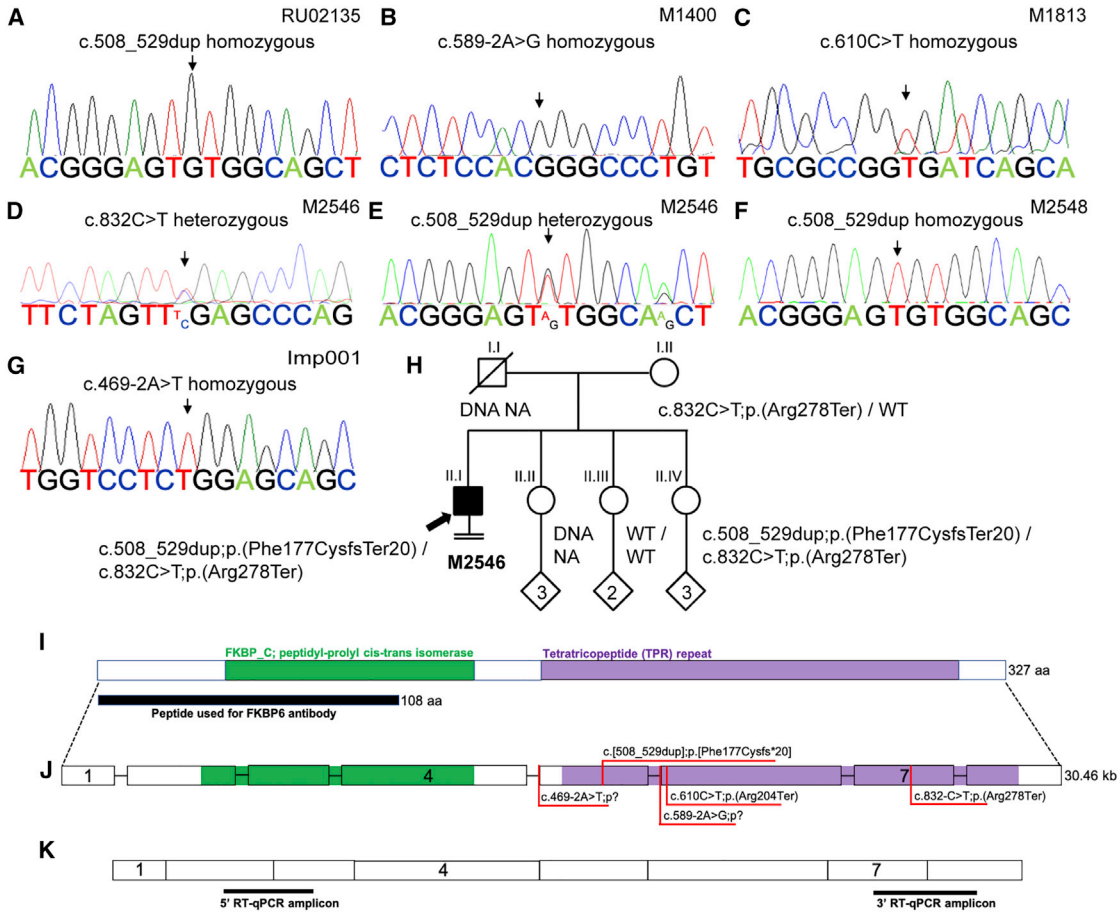

Figure 1. Sanger sequences of identified pathogenic variants in *FKBP6*

(A–G) Electropherograms of identified pathogenic variants in *FKBP6*. The arrow indicates the start of the duplication or the variant.

(A) The 22 base pair duplication c.508_529dup in RU02135.

(B) The homozygous splice acceptor variant c.589−2A>G in M1400.

(C) The homozygous stop-gain variant c.610C>T in M1813.

(D) The heterozygous stop-gain variant c.832C>T in M2546.

(E) The heterozygous 22 base pair duplication c.508_529dup in M2546.

(F) The homozygous 22 base pair duplication c.508_529dup in M2548.

(G) The homozygous splice acceptor variant c.469−2A>T in Imp001.

(H) Pedigree of M2546's family indicating that compound-heterozygosity of these variants causes male infertility but not female infertility.

(I) Structure of FKBP6. FKBP6 has two functional domains: FKBP_C is an inactive peptidyl-proplyl *cis-trans* isomerase domain. The TPR domain is crucial for binding HSP90. The size and relative position of the peptide against which the commercial FKBP6 antibody was raised is indicated by the black bar.

(J) Relative positions of the five identified *FKBP6* variants in order of appearance in the gene: c.469−2A>T (Imp001), c.508_529dup (RU02135, M2548, and M2546), c.589−2A>G (M1400), c.610C>T (M1813), and c.832C>T (M2546). Black numbers indicate exon numbers.

(K) Positions of the amplicons generated by the 5′ and 3′ primer pairs used for RT-qPCR.

likely that both variants have been inherited from their parents following Mendelian rules. According to gnomAD, the stop-gain variant c.832C>T (p.Arg278Ter) has an extremely low frequency of 0.00066%, while no homozygous individuals are listed. Individual M1400 was homozygous for the splice site variant c.589−2A>G (p.?), which is predicted to disrupt the splice acceptor site of exon 6 (Figures 1B, 1J, and S3) and not listed in gnomAD.

This variant abolishes the exon 6 splice acceptor site in *FKBP6* and leads to the activation of two alternative splice sites *in vitro*. The activated splice site in intron 5 further leads to the inclusion of 55 bp from the 3′ end of the intron, including the exchange at c.589−2A>G and results in a premature stop codon due to a frameshift (r.588_589ins589−55_589−1 [p.Ala197GlyfsTer31]). The second alternative splice site is located within exon 6 and leads to the deletion of 28 bp from the 5′ end of the exon resulting in a frameshift and premature stop codon (r.589_616del [p.Ala197HisfsTer18]) (Figure S4A). M1813 was homozygous for the stop-gain variant c.610C>T (p.Arg204Ter), leading to a premature stop codon in exon 6 (Figures 1C and 1J). This variant was found with a frequency of 0.002% in gnomAD with no homozygous individuals listed. Individual Imp001 from the Imperial

Table 1. Genetic and clinical data of infertile men with bi-allelic *FKBP6* variants

Individual	Age, origin	*FKBP6* variant (GRCh37 NM_003602.4)	MAF (gnomAD)	MAF (local controls)	Classification according to ACMG-AMP guidelines	Fertility parameters				Semen analysis results, testicular sperm extraction (TESE), or fine needle aspiration (FNA) outcome
						FSH (U/L)	LH (U/L)	T (nmol/L)	TV (mL)	
RU02135	36 y, the Netherlands	c.[508_529dup]; [508_529dup]; p.[Phe177CysfsTer20]; [Phe177CysfsTer20]	1.48×10^{-4}	6.9×10^{-4}	pathogenic	8.3	2.2	14	19/10	extreme oligozoospermia, all sperm malformed; unsuccessful TESE
M1400	43 y, Syria	c.589−2A>G; (589−2A>G); p.(?); (?)	4×10^{-6}	0	pathogenic	7.7	3.5	13.4	7/14	extreme oligozoospermia, morphology not determined; unsuccessful TESE
M1813	37 y, Brazil	c.610C>T; ;(610C>T); p.(Arg204Ter); (Arg204Ter)	1.78×10^{-5}	0	likely pathogenic	7.7	2.8	18	20/18	azoospermia, TESE not attempted
M2546	28 y, Kyrgyzstan	c.[508_529dup]; [832C>T]; p.[Phe177CysfsTer20]; [Arg278Ter]	1.48×10^{-4}/ 4×10^{-6}	6.9×10^{-4}/0	pathogenic/likely pathogenic	3.9	4.5	18.1	10/12	extreme oligozoospermia, most sperm malformed; unsuccessful TESE
M2548	26 y, Germany	c.508_529dup; (508_529dup); p.(Phe177CysfsTer20); (Phe177CysfsTer20)	1.48×10^{-4}	6.9×10^{-4}	pathogenic	1.8	4.0	18.6	39/23	extreme oligozoospermia, all sperm malformed; unsuccessful TESE
Imp001	28 y, not specified	c.469−2A>T; (469−2A>T); p.(?)(;)(?)	0	0	likely pathogenic	12.4	4	20.2	6/12	extreme oligozoospermia, all sperm malformed; unsuccessful FNA

Abbreviations: y, years; FSH, follicle-stimulating hormone; LH, luteinizing hormone; T, testosterone; TV, testicular volume; TESE, testicular sperm extraction; FNA, fine needle aspiration. Reference values: FSH: 1–7 U/L; LH: 2–10 U/L; T: >12 nmol/L; TV: >12 mL.

cohort was homozygous for a splice site variant c.469−2A>T (p.?) in *FKBP6*, which is predicted to result in a loss of the canonical acceptor splice site of exon 5 (Figures 1G and 1J). Bioinformatic analysis with the ASSP tool identified an alternative splice acceptor site within exon 5 (Figure S5). This variant leads to a skipping of exon 5 *in vitro*, further leading to a frameshift, resulting in a premature stop codon (r.469_588del [p.Glu157GlyfsTer13]) (Figure S4B). No testicular RNA from this proband was available to further analyze the impact of the splice site variant. The variant was absent in the control cohort of proven fathers and mothers and is not listed in gnomAD. A relatedness test (Somalier) for RU02135, M2546, and M2548, who were all identified with exactly the same 22 bp insertion causing a frameshift variant in *FKBP6*, revealed no relatedness between these men.

All five different bi-allelic variants in *FKBP6* observed in this study were assessed as (likely) pathogenic according to the ACMG-AMP criteria (Tables 1 and S2). Since our data support that alterations to the normal functioning of *FKBP6* have a negative impact on male fertility, *FKBP6* reaches a "strong" level of evidence in the context of male infertility in gene validity assessment according to the ClinGen gene validity curation framework (Table S3).

No alternative causes for infertility were revealed after screening the exome sequencing data of RU02135, M1400, M1813, M2546, M2548, and Imp001 for possibly pathogenic variants (stop-, frameshift-, splice site,- and missense variants with a CADD score >25) in 242 genes reported to be related to male infertility (list of genes in the supplemental methods).

Clinical characteristics of affected men

In all men with bi-allelic *FKBP6* variants, very few spermatozoa were observed in the semen, resulting in extreme oligozoospermia, except for M1813 who was azoospermic (Tables 1 and S4). In RU02135, all spermatozoa were morphologically abnormal as they were multiflagellated and had head malformations. In Imp001, a total of 17 abnormal sperm were found many of which had amorphous heads or double or triple tails. Sperm of M2548 were equally multi-flagellated with fragmented and enlarged heads. Since the sperm in their ejaculates did not meet the motility and morphology criteria for MAR, RU02135, M1400, M1813, M2546, and M2548 underwent a testicular biopsy with the aim of obtaining viable sperm via a TESE procedure. Imp001 underwent fine needle aspiration (FNA). None of these procedures were successful in retrieving viable sperm cells. No testicular tissue was available for further analyses from M1813. The original pathology report of M1813's testis tissue made note of an arrest of germ cells during meiosis. Clinical parameters of all individuals are listed in Tables 1, S4, and S5.

As variants in *FKBP6* have been described in association to multiple sclerosis,[53,54] we investigated the medical files of the six affected individuals for neurological impairments. RU02135, M1813, M2546, M2548, and Imp001 had no history of neurological disease and no obvious neurological abnormalities were recorded. During his childhood in Syria, M1400 experienced questionable signs of paralysis of which there are no reports available. These symptoms did not return later in life.

FKBP6 appears in late spermatocytes and localizes to nuages but not to the synaptonemal complex

To understand the putative functions of FKBP6 during spermatogenesis, we performed immunofluorescence (IF) staining. We probed control testicular sections with a commercially available antibody raised against aa 1–108 of the canonical FKBP6 (Figure 1I, Subjects and methods). We combined this staining with an SYCP3 staining, a component of the SC. FKBP6 signal accumulated in a subset of spermatocytes as a non-homogeneous punctate cytoplasmic staining. Presence of FKBP6 was limited to spermatocytes showing prominent and long SYCP3 stretches and DAPI bright compartmentalized heterochromatin, all characteristics typical for spermatocytes in pachynema to diplonema (Figures 2A–2C and S6A–S6L). Signal was predominantly detected in spermatocytes, with some early round spermatids displaying a low level of staining pattern (Figure S6K). No staining of spermatogonia was observed (Figures S6A–S6L).

We did not observe a nuclear localization for FKBP6. To exclude the possibility of technical aspects precluding SC localization in our sections, we generated nuclear spreads of testicular cells from control samples (n = 3). In order to include a positive control for the FKBP6 antibody staining, we also prepared spreads without the presence of the cytoplasm disrupting soap Triton X-100. Although the SC was identified by SYCP3 staining, we were not able to detect FKBP6 localization to this structure (Figures 2D–2F and S6M–S6AD). Since the cytoplasmic staining of FKBP6 showed granules, we investigated whether some of these could be nuages, germ cell-specific cytoplasmic structures that are sites of piRNA pathway activity.[20] Different types of nuages exist also in human germ cells.[55] We therefore determined FKBP6 localization in human control samples in relation to PIWIL1, whose ortholog is a known interactor of Fkbp6 in mice.[29] A clear overlap in localization between these two proteins was observed for the larger FKBP6 granules (Figures 2G–2I).

Many piRNA genes become expressed at mid meiosis through binding of the transcription factor MYBL1,[56] which also accumulates in the promoter region of *FKBP6* in human spermatocytes.[56] We performed a double staining with antibodies against MYBL1 and FKBP6 (Figures 2J–2L). By counting positive spermatocytes, we found that all spermatocytes that stained positive for FKBP6 also did so for MYBL1 ($n_{contols} = 2$, $n_{cells} = 200$). Conversely, however, roughly 10% of all MYBL1-positive nuclei did not exhibit FKBP6 staining (Table S6).

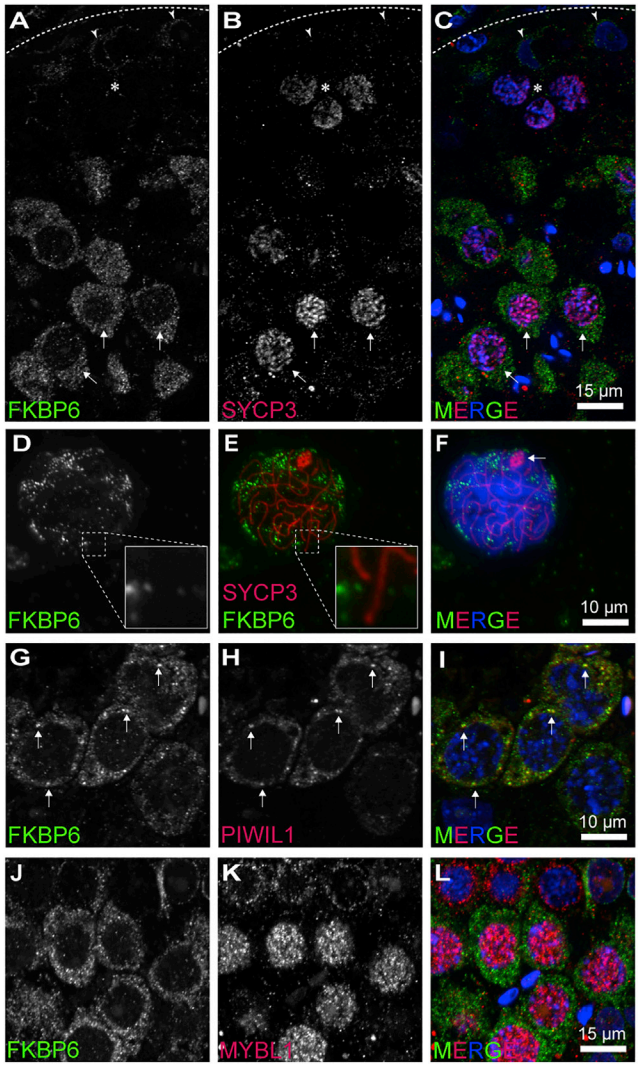

Figure 2. Localization and accumulation of FKBP6 in normal spermatogenesis

Antibody staining on testis sections (A–C, G–L) and nuclear surface spreads (D–F) from a control subject with complete spermatogenesis.

(A–C) The localization and timing of accumulation of FKBP6 was analyzed by combining antibody stainings for FKBP6 (A) and SYCP3 (B), a marker of the synaptonemal complex (SC). DNA was stained with DAPI (C, merge). FKBP6 accumulation was mainly limited to spermatocytes that had a clear build-up of the SC (arrows indicate examples). Earlier spermatocytes (indicated by asterisk) lacked staining. Faint signal outlining Sertoli cells was frequently observed (arrowhead). Dotted line indicates position of basal lamina. See Figure S6 for additional images.

(D–F) Nuclear surface spreads were stained for FKBP6 (D), SYCP3 (E, merged with FKBP6), and DAPI (F, merge). No localization of FKBP6 to the SC was observed. The enlarged region is indicated in (D) and (E). The arrow in (F) indicates the XY body of which the SYCP3 staining pattern is indicative of a late meiotic stage. See Figure S6 for additional images.

(G–I) Antibody double staining for FKBP6 (G) and the piRNA pathway protein PIWIL1 (H). DNA was stained with DAPI (I, merge). Arrows indicate occasions of overlapping signals for FKBP6 and PIWIL1.

(J–L) Antibody double staining for FKBP6 (J) and the transcription factor MYBL1 (K). DNA was stained with DAPI (L, merge). FKBP6 is detected after nuclear appearance of the transcription factor MYBL1.

FKBP6 expression is lost in infertile men RU02135, M1400, M2546, and M2548

To determine whether the identified variants affect FKBP6 expression or localization, we repeated the IF staining for FKBP6 on testicular sections from these men. Cytoplasmic staining was absent from germ cells, also late spermatocytes. A weak staining outlining Sertoli cells was frequently observed (Figures 3A–3L). Since FKBP6 is not expressed in human Sertoli cells, this signal likely represents unspecific background staining[57,58] (Figure S6). To verify these results at mRNA level, we performed RT-qPCRs on RNA extracted from FFPE tissue of RU02135 and from snap frozen testicular tissue of M1400, M2546, and M2548. Two primer sets were designed that, when combined, detected all seven isoforms of *FKBP6* (Figure 1K, supplemental methods). For all four men, a significant reduction of *FKBP6* transcripts was observed ($p = 0.008$; t test, Figures 3M, 3N, and S7A–S7G). To verify that this reduction was not due to a significant loss of late spermatocytes, we also performed RT-qPCR experiments for *SYCP3* and *PIWIL1*. These data indicate that this is indeed not the case (Figures S7H–S7K).

Bi-allelic pathogenic variants in *FKBP6* cause germ cell loss at various stages during spermatogenesis

To determine the overall effect of FKBP6 loss on spermatogenesis, we assessed testicular histology by analyses of H&E-stained tissue from four men: RU02135, M1400, M2546, and M2548. For Imp001, PAP-stained cytological preparations were available with cells obtained via FNA. No testicular histology was available for M1813.

In all available histologies, the most progressed cell type present in cross sections of seminiferous tubules were quantified. This analysis revealed that in all four men the most progressed germ cells were round spermatids. Importantly, no elongated spermatids were observed in any of the individuals (Figure 4; Table S7). A difference in the prevalence of tubules with round spermatids between these four men was noted. The highest percentage was observed in RU02135 (62%) whereas other individuals showed much lower values (between 30% and 40%). In these individuals, tubules that showed MeiA were much more abundant (Figure 4M). In the PAP-stained cytological preparations from Imp001, we failed to identify elongated spermatids (Figures 4K and 4L). However, round spermatids and pyknotic cells that resembled such cells in the H&E sections of the other four men were observed.

Germ cell loss in absence of FKBP6 occurs in late meiosis up to early spermiogenesis

Our histological analyses indicated that germ cells are lost during either meiosis or spermiogenesis (Figure 4M). In *Fkbp6* KO (*Fkbp6*$^{-/-}$) mice, germ cells become arrested during pachytene.[31] To determine how the spermatogenic failure observed in men with bi-allelic *FKBP6* variants compares with this observation, we performed an extensive

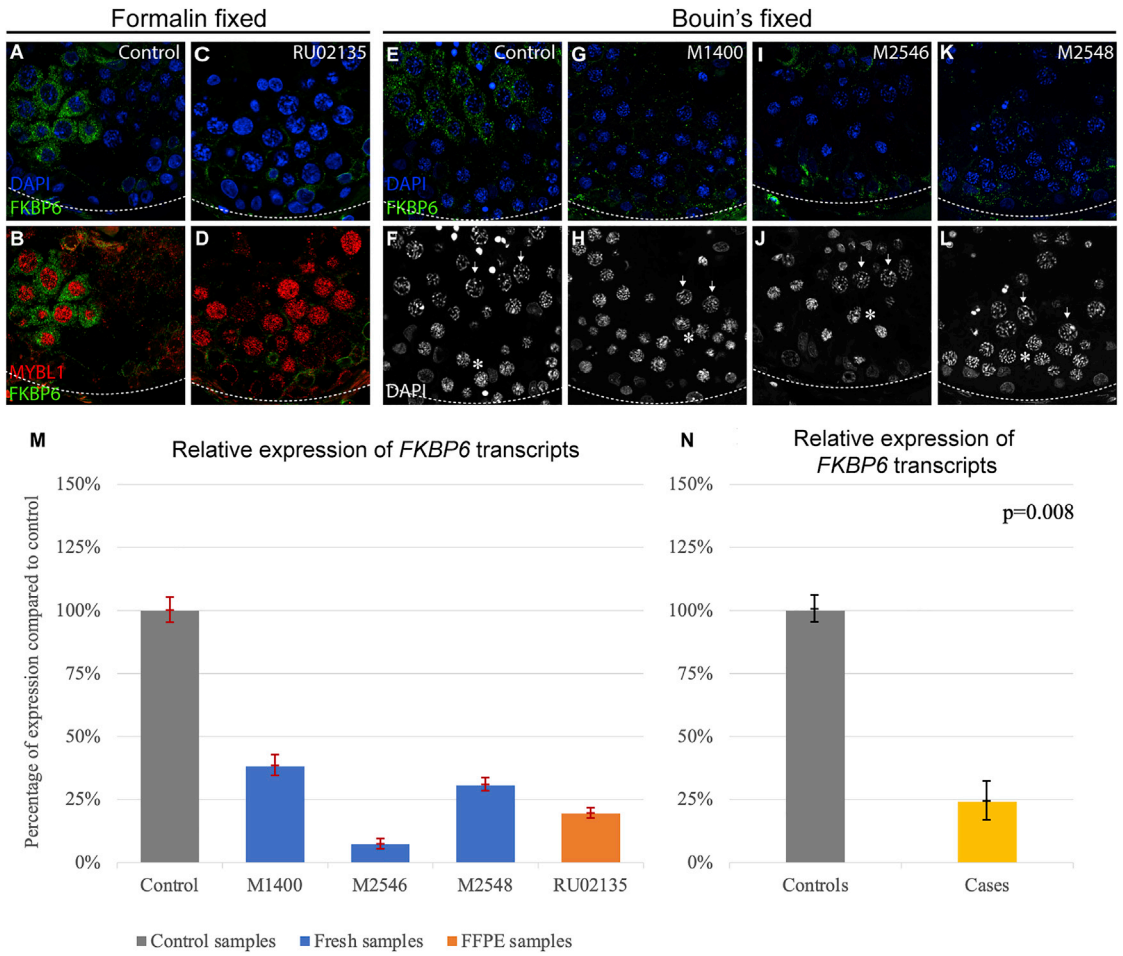

Figure 3. Expression of *FKBP6* is lost in RU02135, M1400, M2546, and M2548

(A–L) Antibody staining for FKBP6 on testicular sections from control subjects (A, B, E, F), RU02135 (C, D), M1400 (G, H), M2546 (I, J), and M2548 (K, L).

(A–D) Formalin-fixed samples. FKBP6 is shown in green, MYBL1 (a marker for late spermatocytes) in red, and DNA in blue. In control tissue (A, B), a clear cytoplasmic signal for FKBP6 is observed in late spermatocytes. Such signal is absent from germ cells from RU02135 (C, D).

(E–L) Bouin's fixed material. Epithelium in which an early and late cohort of spermatocytes are present are shown (indicated with asterisks and arrows, respectively, in F, H, J, L). The presence of two meiotic cohorts indicates the older cohort to be late spermatocytes. FKBP6 is shown in green and DNA in blue (E, G, I, K) or white (F, H, J, L). In control tissue (E), a clear cytoplasmic signal for FKBP6 is observed in late spermatocytes. Such signal is absent from germ cells from M1400 (G), M2546 (I), and M2548 (K). Dotted line indicates the position of the basal lamina.

(M and N) Relative expression of *FKBP6* gene transcripts in testicular tissue was evaluated by RT-qPCR. Relative expression of *FKBP6* is shown as a percentage of expression in a grouped control sample. Two amplicons, located 5′ and 3′ of *FKBP6* transcripts, were used for overall gene expression evaluation. Results for both amplicons were combined, averaged, and shown in this figure. Red error bars represent technical variability of three RT-qPCR reactions for each case-control pair, while black error bars indicate biological variability among case and control samples.

(M) *FKBP6* expression levels are significantly decreased in all case samples.

(N) Grouped case samples represent significant downregulation of *FKBP6*.

analysis of meiosis and spermiogenesis in affected men (see Subjects and methods).

We analyzed meiotic cells in testis sections of RU02135 (formalin fixed) and M1400 (Bouin's fixed) by performing IF against γH2AX, a general marker for meiotic progression and apoptosis (Figures S8A–S8O). We identified an increase in the proportion of apoptotic MPI cells in both individuals (RU02135 versus controls: 0.049 versus 0.019; p value = 0.001; M1400 versus controls: 0.069 versus 0.0095; p value = 0.001; chi-squared test; Figure 5A, Tables S8 and S9). The quantification of cell numbers per meiotic sub-stages indicates that cell loss occurs during late meiosis (Figure 5A, Tables S8 and S9). When combining staining for γH2AX and H3S10ph to identify apoptotic metaphases, we found their number to be increased in both affected men compared to the control subjects (RU02135 versus controls: 0.064 versus 0.009; p value = 0.001; M1400 versus controls: 0.149 versus 0.009; p value = 0.001; chi-squared test; Figures 5B, S8P, and S8Q, Tables S10 and S11).

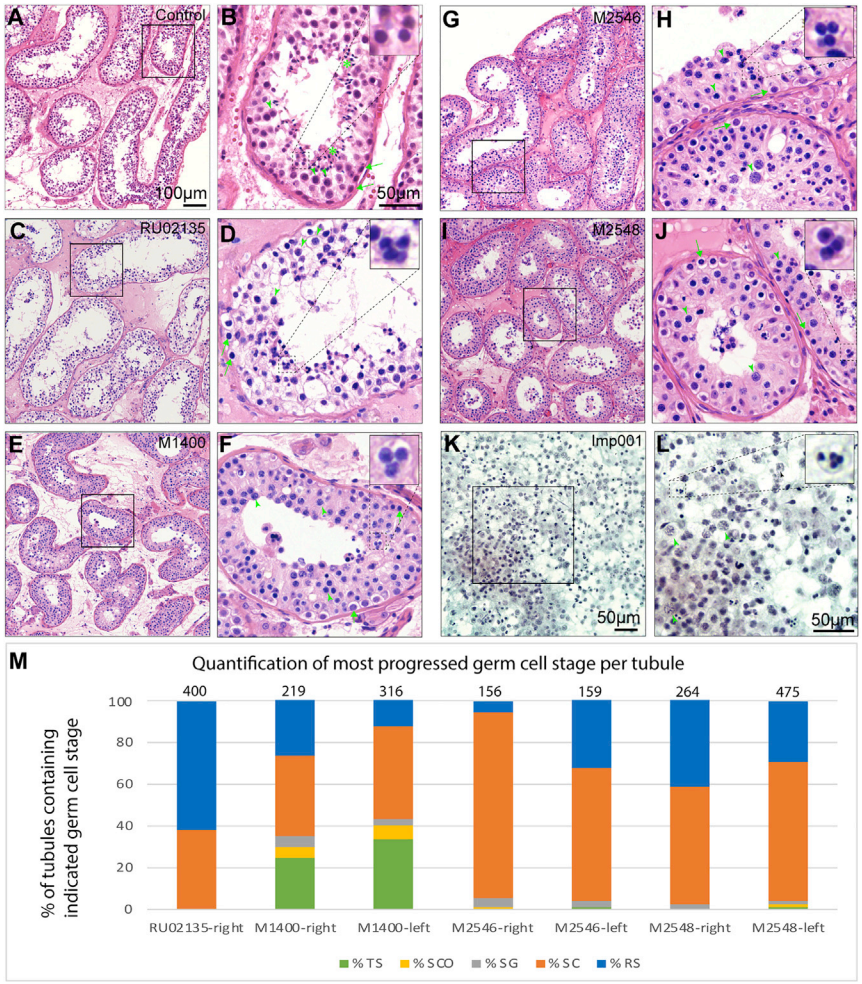

Figure 4. Testicular histology in a control subject and in the affected men

(A–L) H&E-stained testicular sections of a control subject with complete spermatogenesis (A, B), RU02135 (C, D), M1400 (E, F), M2546 (G, H), M2548 (I, J), and PAP-stained air-dried cell spreads of testicular cell suspension of Imp001 (K, L) are shown. Black rectangles indicated in the left panel are depicted enlarged in the right panel. Examples of the main stages of germ cell maturation during spermatogenesis are indicated in each image: spermatogonia (green arrow), spermatocytes (green arrowhead), round spermatids (depicted enlarged in each right panel; location of this enlarged image is indicated by dashed black lines), and elongated spermatids (green asterisk, only present in control panel B).

(M) Quantification of most progressed germ cell stage per tubule expressed as a percentage. The number of assessed tubules is indicated on top of the individual bar plots. When tissue of both testes was available, both are shown. Abbreviations: TS, tubular shadows; SCO, Sertoli cell only; SG, spermatogonia; SC, spermatocytes; RS, round spermatids.

In male *Fkbp6*$^{-/-}$ mice, a failure to finalize synapsis underlies the meiotic arrest.[31] To determine whether this is also the case in human spermatocytes lacking FKBP6, we assessed pachytene cells for the presence of additional γH2AX domains which indicate asynapsis.[59] We did not observe cells in which such additional domains were present (Figures 5C–5E). To investigate whether loss of FKBP6 results in a more subtle change of γH2AX staining pattern, we quantified whether pachytene spermatocytes showed an increase of additional small specks in addition to the XY body. No difference between the affected men and the control subjects was observed (Figures S8R and S8S, Tables S12 and S13).

To determine the timing of the spermiogenesis arrest, we analyzed the formation of the acrosome. To this end, we stained sections with peanut agglutinin (PNA)[60] and an antibody against GORASP2, a component of the Golgi apparatus. For all four men (RU02135, M1400, M2546, and M2548), most spermatids showed an acrosome as a granule that resided at one pole of the spermatid (Figures 5F–5M and S9A–S9I). In addition, acrosomal material was frequently present as aggregates (Figures S9A–S9I). Very infrequently, there was an indication of spreading of the acrosome over the nucleus (Figure S9C). Altogether, these results show that the onset of germ cell loss coincides with the appearance of FKBP6 in control subjects and occurs in late meiosis and early spermiogenesis. Virtually no progression beyond the first stage of spermiogenesis was observed.

Loss of FKBP6 affects piRNA production

Next, we investigated whether loss of FKBP6 affects piRNA production. For M1400, M2546, and M2548 and corresponding control subjects, RNA was isolated from snap frozen testis material (supplemental methods). RNA for RU02135 and the control subject was isolated from FFPE material. Small RNAs were sequenced according to previously published protocols.[6] RNA from RU02135 and M1400 was sequenced with Illumina's MiSeq, while RNA from M2546 and M2548 was sequenced with NovaSeq, resulting in a higher sequencing depth in the latter two samples and respective controls.

A first analysis of read counts from piRNAs of 25–45 nucleotides (nt) length identified a significant reduction in piRNAs from M1400 but not in piRNAs from RU02135, M2546, and M2548 ($p = 0.01$, $p = 0.64$, $p = 0.21$, and $p = 0.21$, respectively, t test; Figures 6A–6D). Because of the known interaction between FKBP6 and PIWIL1,[29] we next analyzed whether loss of FKBP6 specifically affected PIWIL1-associated piRNAs, which are characterized by a length of ~30 nt.[52] In M1400, M2546, and M2548 we

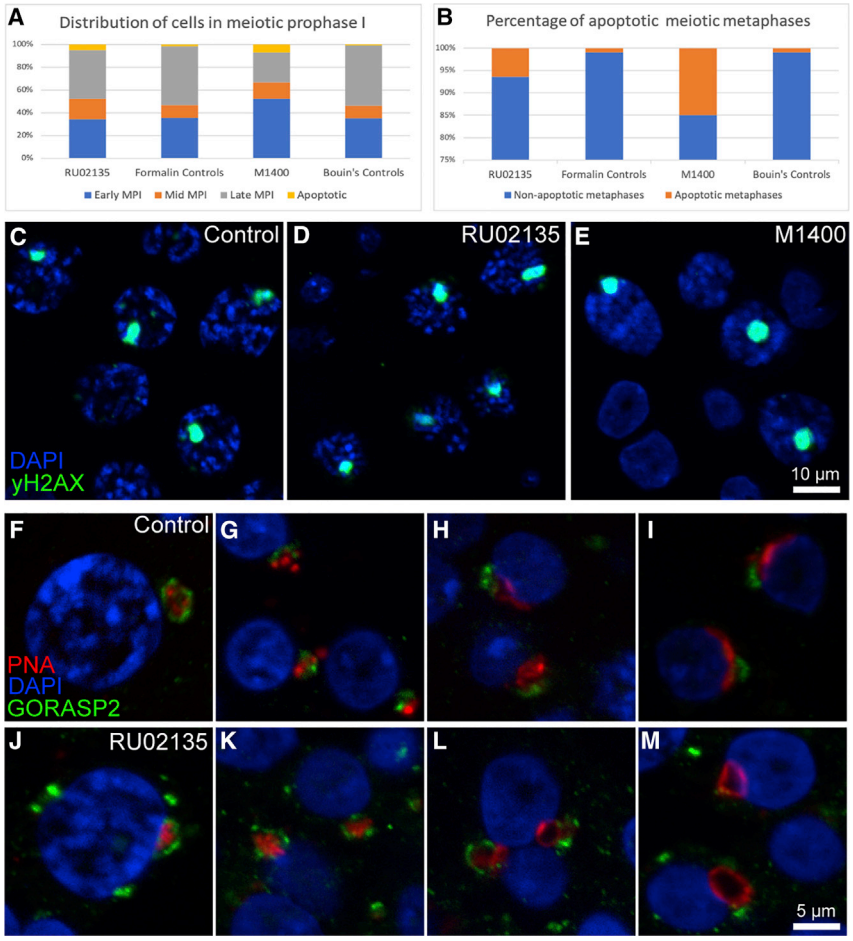

Figure 5. Effects of loss of *FKBP6* on meiosis and spermiogenesis

(A) Graph depicting the effect of the *FKBP6* variants on the distribution of cells in meiotic prophase I (MPI) and proportion of apoptotic meiotic cells. MPI was divided in early, mid, and late according to γH2AX staining patterns. A significant change in the mid and late fractions was observed in both RU02135 and M1400. In both men an increase in the number of apoptotic cells was observed.

(B) Graph depicting the percentage of apoptotic meiotic metaphases. In both men an increase of apoptotic meiotic metaphases was observed.

(C–E) Antibody staining against γH2AX (green) of control (C), RU02135 (D), and M1400 (E) sections. DAPI is used as DNA stain. The XY body stains prominent for γH2AX in all three samples. No additional γH2AX-positive domains were observed in RU02135 and M1400.

(F–M) Triple staining against the acrosome (PNA, red), Golgi (anti-GORASP2, green), and DNA (DAPI, blue) on testis sections from a control subject with complete spermatogenesis (F–I) and RU02135 (J–M). In spermatocytes (F, J) and early round spermatids (G, K), no difference between the control subject and RU02135 was observed. While spreading of the acrosome over the nucleus was observed in the control subject (H, I), this was virtually never observed for RU02135, in which the acrosome remained a sphere (L). Increasing sizes of these spheres were observed, likely reflecting increasing maturation (M).

indeed observed a significant loss of piRNAs ranging from 28 to 32 nt ($p = 0.03$, $p = 0.05$, and $p = 0.05$, respectively, t test; Figures 6B–6D). In RU02135 no significant loss of 28–32 nt piRNAs was observed ($p = 0.42$; t test; Figure 6A).

Loss of FKBP6 does not induce LINE-1 upregulation

Upregulation of LINE-1 transposons is a hallmark of piRNA pathway malfunctioning in mice.[61] To determine whether this is also the case in humans, we assessed LINE-1 expression by staining against L1ORF1p. In wild-type mice spermatogenesis, L1ORF1p accumulates solely in germ cells during early meiosis.[12,16] We found that in human spermatogenesis L1ORF1p accumulation was very similar: it was predominantly observed in meiotic cells and increased during mid-late meiosis (Figures 7A–7D and S9J–S9M). We did not see an increase in L1ORF1p signal in RU02135, M1400, M2546, and M2548 compared to the control tissue (Figures 7E–7T). To determine whether this observation is specific for our *FKBP6* individuals or a general feature of piRNA pathway functionality in human spermatogenesis, we repeated this staining in testis sections from a man with severe piRNA impairment due to pathogenic homozygous variant in *PNLDC1*.[6] In these germ cells again no increase of L1ORF1p accumulation was observed (Figures 7U–7X). Potentially, LINE-1 upregulation still occurs but regulation at a translational level precludes an increase of L1ORF1p. To verify this, we determined LINE-1 mRNA levels via RT-qPCR. A previously published assay for LINE-1 RT-qPCR was used which is based on 5′ and 3′ LINE-1 amplicons.[62] In none of the examined samples did we find an increase of LINE-1 transcripts (Figures 7Y, 7Z, and S10). These results confirm our IF results and, taken together, suggest that loss of FKBP6 or PNLDC1 and their accompanied reduction in piRNA levels do not induce LINE-1 overexpression in human spermatogenesis.

Discussion

In this study, we show that FKBP6 is involved in the production of piRNAs during spermatogenesis and that its loss leads to spermatogenic failure. Women do not seem to be affected by bi-allelic pathogenic variants in *FKBP6*, which matches the fertile phenotype observed in female *Fkbp6*$^{-/-}$ rodents. Concerning the variants identified in RU02135, M1400, M2546, and M2548, we were able to show that FKBP6 mRNA and protein levels were severely

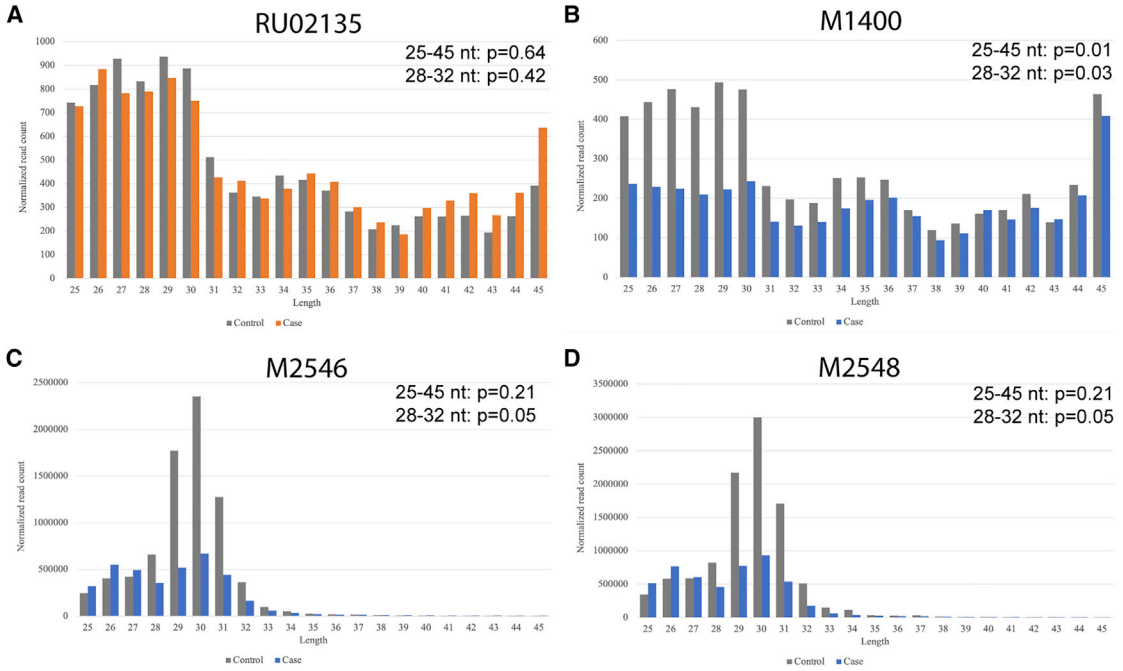

Figure 6. piRNA pathway functionality in *FKBP6* cases

Read length distribution of piRNAs in (A) RU02135, (B) M1400, (C) M2546, and (D) M2548. The number (Y axis) of piRNA molecules from a specific length (X axis) was determined. RNA obtained from FFPE material is shown in orange and in blue when obtained from snap-frozen material. A significant reduction of piRNA molecules of 28–32 nucleotides was observed for M1400, M2546, and M2548 when compared to the relative control subjects. No significant reduction was observed for RU02135.

reduced. The splice site variant detected in M1400 activates two different splice sites, which both lead to a premature stop codon due to a frameshift. The splice variant in Imp001 leads to the skipping of exon 5, and thus affects FKBP6's TPR domain, which enables the interaction with Hsp90, which is crucial for its function in the piRNA pathway.[24,28] The stop-gain variant in M1813 is predicted to result in nonsense-mediated decay.

While most affected individuals in this study were diagnosed with extreme oligozoospermia, M1813 presented with azoospermia. This is not unusual as both conditions form a continuum and can be found in the same individual in repeated analyses.[63] Moreover, slightly varying phenotypes are also known from other male infertility genes such as *AR* and *M1AP*.[63] The rare presence of spermatozoa in the semen in some men might be due to polygenic or environmental factors.

In mice, Fkbp6 has been reported to localize to the SC.[31] However, we were unable to confirm this localization, suggesting that FKBP6 is not involved in SC formation in humans. Absence of FKBP6 from the SC could explain the difference in meiotic phenotype between men and mice. While mouse spermatocytes fail to finalize synapsis, we show that this is not the case for human spermatocytes. Our results, therefore, suggest that unlike in male *Fkbp6*$^{-/-}$ mice, asynapsis is not the underlying cause of spermatocyte loss in men with pathogenic variants in *FKBP6*.

Increased germ cell loss marked by apoptotic spermatocytes and metaphases is observed from late meiosis in affected men, coinciding with the appearance of FKBP6 in control subjects. Interestingly, in mouse models of the piRNA factors *Piwil1* and *Mael,* an increased loss of meiotic metaphases has also been described.[16,64] Germ cells of affected men, which were able to complete meiosis, virtually all arrest at the onset of spermiogenesis during the Golgi-phase of acrosome formation. An identical arrest is also observed for several piRNA pathway mutants in mice,[20] notably also for two known Fkbp6 interactors: Tdrd1 and Piwil1.[65,66]

The sequencing results of piRNAs obtained from testicular tissue of RU02135, M1400, M2546, and M2548, showed notable differences. While piRNA levels were greatly reduced in M1400, M2546, and M2548, piRNA levels in RU02135 were not affected. Notably, RU02135 and M2548 share an identical variant, which makes a technological explanation more likely. Possibly the difference in preservation of the analyzed tissue plays a role, because RNA from RU02135 was obtained from FFPE tissue, while for the other samples snap frozen material was available. Since the three samples for which unfixed material was used all showed a significant reduction of piRNAs of 28–32 nt length, we assume a role of FKBP6 in piRNA production. More specifically, the reduction of piRNAs of this length is suggestive of an interaction between FKBP6 and PIWIL1, which has been reported in mice.[29]

The massive overexpression of LINE-1 TEs during meiosis is a hallmark of piRNA pathway dysregulation and the likely cause of infertility in many mouse mutants with an impaired piRNA pathway.[61] In this study, however,

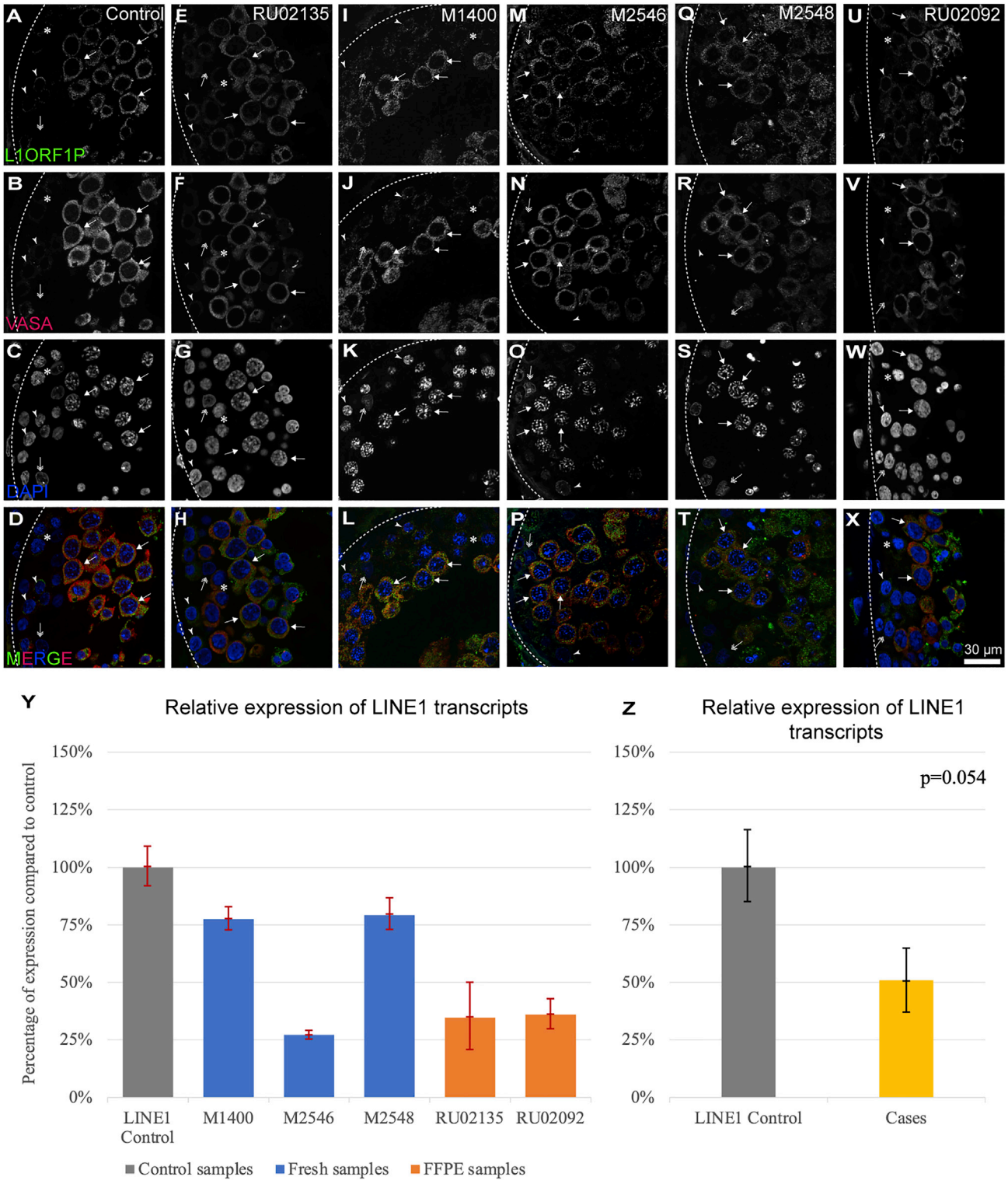

Figure 7. Loss of *FKBP6* or *PNLDC1* does not increase LINE-1 expression

Antibody stainings for L1ORF1p (green) and germ cell marker VASA (red) were used to determine the effect of *FKBP6* and *PNLDC1* variants on LINE-1 expression. DNA was stained with DAPI (blue). In each panel examples of the following cell types are indicated when present: spermatogonia (arrowheads), early spermatocytes (asterisks), late spermatocytes (arrows), and Sertoli cells (double-headed arrows).

(A–D) Control tissue. Expression of L1ORF1p is restricted to VASA-positive cells. Low levels of L1ORF1p staining was observed in spermatogonia and early spermatocytes. Sertoli cells lacked staining. An increase of L1ORF1p signal was observed in mid-late spermatocytes. (E–X) Sections of men affected by variants in *FKBP6* (E–T) or *PNLDC1* (U–X). No increase in L1ORF1p staining was observed in RU02135 (E–H), M1400 (I–L), M2546 (M–P), or M2548 (Q–T). In addition, loss of piRNA pathway factor PNLDC1 (U–X) did not result in increased L1ORF1P levels.

(legend continued on next page)

we show that loss of FKBP6 and reduced piRNA levels do not result in increased L1ORF1p expression. We extend these findings to PNLDC1, another piRNA factor whose loss greatly diminishes piRNA levels.[6] While loss of Pnldc1 in male mice results in vastly increased L1ORF1p accumulation during meiosis,[67] we observed no increase of L1ORF1p signal in this individual. This apparent lack of LINE-1 upregulation could suggest that LINE-1 DNA methylation was not affected during fetal development or has been restored since. Alternatively, FKBP6 and PNLDC1 are not involved in the production of LINE-1-directed pre-pachytene piRNAs during human male meiosis. The latter assumption is supported by the observation that expression of *FKBP6* coincides with the appearance of pachytene piRNAs.[56] These piRNAs are mainly involved in regulation of protein coding genes in mice. Their loss does not affect LINE-1 expression[8,15–17,68] and results in a RsA.[16,68] The spermatogenetic arrests we observed in our individuals are therefore likely a consequence of the dysregulation of the mRNA translational program due to loss of pachytene piRNAs.

Our study elucidates FKBP6's function in humans and underlines its importance for human male fertility. As *FKBP6* immediately reaches a "strong" level of evidence in the context of male infertility, according to the ClinGen classification, it is directly applicable for clinical diagnostics. This will help to provide affected men with a causal diagnosis. In all six affected men, the ejaculated spermatozoa were not suitable for utilization in MAR and no sperm were gained via surgical methods for this purpose either. Our findings indicate that the prospect of successful testicular biopsy and subsequent TESE for men with bi-allelic (likely) pathogenic variants in *FKBP6* is minimal. Affected individuals can be counseled accordingly before testicular biopsy, helping to prevent unnecessary surgical procedures.

Consortia

Members of the Genetics of Male Infertility Initiative (GEMINI) consortium are Donald F. Conrad, Liina Nagirnaja, Kenneth I. Aston, Douglas T. Carrell, James M. Hotaling, Timothy G. Jenkins, Rob McLachlan, Moira K. O'Bryan, Peter N. Schlegel, Michael L. Eisenberg, Jay I. Sandlow, Emily S. Jungheim, Kenan R. Omurtag, Alexandra M. Lopes, Susana Seixas, Filipa Carvalho, Susana Fernandes, Alberto Barros, João Gonçalves, Iris Caetano, Graça Pinto, Sónia Correia, Maris Laan, Margus Punab, Ewa Rajpert-De Meyts, Niels Jørgensen, Kristian Almstrup, Csilla G. Krausz, and Keith A. Jarvi. The affiliations can be found in the supplemental data.

Data and code availability

All variants have been submitted to ClinVar (SCV002507290, SCV002507291, SCV002507292, SCV002507294, SCV002507295) and will be available after 11/12/22. The exome-sequencing data of RU02135 and RU02092 have been deposited in the European Genome-phenome Archive (EGA) under the accession code EGAD00001007862, under the identifiers Proband_163 and Proband_152. Access can be granted upon reasonable request for academic use within the limitations of the provided informed consent by the corresponding author upon acceptance. The request will be reviewed by the Newcastle University Male Infertility Genomis Data Access Committee. After approval, the requesting researcher will be obliged to sign a data access agreement. Exome-sequencing data of men from the MERGE and Imperial cohorts have not been deposited in a public repository (because the research participant's consent did not include this) but are available from the corresponding author on request.

Supplemental information

Supplemental information can be found online at https://doi.org/10.1016/j.ajhg.2022.09.002.

Acknowledgments

We are grateful for the participation of all affected individuals and their family members in this study. We thank Annette Schenk and Lara Renssen for technical and organizational support (Radboud University Medical Center). We thank Joachim Wistuba (University Hospital Münster) and Susana de Sousa Lopes (Leiden University Medical Center) for thoughtful discussions. This project was funded by The Netherlands Organization for Scientific Research (918-15-667) to J.A.V. as well as an Investigator Award in Science from the Wellcome Trust (209451) to J.A.V., a grant from the Catherine van Tussenbroek Foundation to M.S.O., a grant from Merck to R.S. and the German Research Foundation Clinical Research Unit "Male Germ Cells" (DFG, CRU326) to F.T., by independent financial support by the Novo Nordisk Foundation (grant# 0069913 to K.A.), the Independent Research Fund Denmark (grant# 1030-00381B to K.A.), and the Svend Andersen Foundation (grant# 84 - A.08 to K.A.) to K.A., by grants from the National Institutes of Health of the United States of America (R01HD078641 and P50HD096723) to D.F.C., and by research grant BB/V011251/1 from Biotechnology and Biological Sciences Research Council to A.S. P.L. is supported by the Excellence Program of Radboud University and by research grant MOP-44050 from the Canadian Institutes of Health Research. H.G.L. is supported by MRC Core Funding (MC- A6525QA10) and the National Institute for Health Research (NIHR) Imperial Biomedical Research Centre (BRC). C.N.J. is supported by the NIHR and BRC.

Author contributions

G.W.v.d.H. designed and coordinated the study. C.G. and M.S.O. analyzed exome-sequencing data of RU02135 and identified the

(Y–Z) Relative expression of LINE-1 transcripts is shown as a percentage of expression in a control subject. An RT-qPCR assay for LINE-1 expression, which uses two primer sets, was employed to determine LINE-1 expression. Results for both amplicons were combined, averaged, and are shown in this figure. Red error bars represent technical variability of three RT-qPCR reactions for each case-control pair, while black error bars indicate biological variability among case and control samples. (Y) No significant change of overall LINE-1 expression was observed in samples of affected men. (Z) All samples of affected men grouped, represent no significant difference in overall LINE-1 expression when compared with control subjects.

index case. G.W.v.d.H. performed immunofluorescence stainings, imaging, and testicular cell quantifications. I.G., R.S., L.N., K.A., and D.F.C. performed small RNA sequencing and data analysis. I.G., R.S., and K.A. performed RT-qPCRs and data analysis. P.L. provided technical assistance. C.D., H.G.L., E.B.S., C.N.J., and A.S. identified proband Imp001 and assembled corresponding data. C.H.P.G. and T.F.A. assembled data on M1813. M.J.W. did gene and variant assessment. M.J.W., N.R., B.S., S.K., and F.T. provided data and materials of M1400, M2546, and M2548. A.K.D. performed the minigene assays. K.D., R.M.S., and L.R. assembled data of RU02135. M.J.X. performed statistical analyses of immunofluorescence quantifications. M.J.X., D.F.C., J.A.V., and F.T. were involved in conceptualizing the replication studies. The first draft of the manuscript was prepared by M.J.W. and G.W.v.d.H. All authors contributed to the final version and approved it.

Declaration of interests

C.N.J. has an Investigator-led grant from Logixx Pharma Ltd, UK.

Received: May 15, 2022
Accepted: September 1, 2022
Published: September 22, 2022

References

1. Tüttelmann, F., Ruckert, C., and Röpke, A. (2018). Disorders of spermatogenesis: perspectives for novel genetic diagnostics after 20 years of unchanged routine. Med. Genet. *30*, 12–20.
2. Gil-Salom, M., Minguez, Y., Rubio, C., Ruiz, A., Remohi, J., and Pellicer, A. (1996). Intracytoplasmic sperm injection: a treatment for extreme oligospermia. J. Urol. *156*, 1001–1004.
3. Wyrwoll, M.J., Rudnik-Schöneborn, S., and Tüttelmann, F. (2021). Genetic counseling and diagnostic guidelines for couples with infertility and/or recurrent miscarriage. Medizinische Genetik *33*, 3–12.
4. McLachlan, R.I., Rajpert-De Meyts, E., Hoei-Hansen, C.E., de Kretser, D.M., and Skakkebaek, N.E. (2007). Histological evaluation of the human testis–approaches to optimizing the clinical value of the assessment: mini review. Hum. Reprod. *22*, 2–16.
5. Xavier, M.J., Salas-Huetos, A., Oud, M.S., Aston, K.I., and Veltman, J.A. (2021). Disease gene discovery in male infertility: past, present and future. Hum. Genet. *140*, 7–19.
6. Nagirnaja, L., Mørup, N., Nielsen, J.E., Stakaitis, R., Golubickaite, I., Oud, M.S., Winge, S.B., Carvalho, F., Aston, K.I., Khani, F., et al. (2021). Variant PNLDC1 , Defective piRNA Processing, and Azoospermia. N. Engl. J. Med. *385*, 707–719.
7. Ozata, D.M., Gainetdinov, I., Zoch, A., O'Carroll, D., and Zamore, P.D. (2019). PIWI-interacting RNAs: small RNAs with big functions. Nat. Rev. Genet. *20*, 89–108.
8. Dai, P., Wang, X., Gou, L.-T., Li, Z.-T., Wen, Z., Chen, Z.-G., Hua, M.-M., Zhong, A., Wang, L., Su, H., et al. (2019). A Translation-Activating Function of MIWI/piRNA during Mouse Spermiogenesis. Cell *179*, 1566–1581.e16.
9. Hasuwa, H., Iwasaki, Y.W., Au Yeung, W.K., Ishino, K., Masuda, H., Sasaki, H., and Siomi, H. (2021). Production of functional oocytes requires maternally expressed PIWI genes and piRNAs in golden hamsters. Nat. Cell Biol. *23*, 1002–1012.
10. Roovers, E.F., Rosenkranz, D., Mahdipour, M., Han, C.-T., He, N., Chuva de Sousa Lopes, S.M., van der Westerlaken, L.A.J., Zischler, H., Butter, F., Roelen, B.A.J., and Ketting, R.F. (2015). Piwi Proteins and piRNAs in mammalian oocytes and early embryos. Cell Rep. *10*, 2069–2082.
11. Reuter, M., Berninger, P., Chuma, S., Shah, H., Hosokawa, M., Funaya, C., Antony, C., Sachidanandam, R., and Pillai, R.S. (2011). Miwi catalysis is required for piRNA amplification-independent LINE1 transposon silencing. Nature *480*, 264–267.
12. Di Giacomo, M., Comazzetto, S., Saini, H., De Fazio, S., Carrieri, C., Morgan, M., Vasiliauskaite, L., Benes, V., Enright, A.J., and O'Carroll, D. (2013). Multiple epigenetic mechanisms and the piRNA pathway enforce LINE1 silencing during adult spermatogenesis. Mol. Cell *50*, 601–608.
13. Carmell, M.A., Girard, A., van de Kant, H.J.G., Bourc'his, D., Bestor, T.H., de Rooij, D.G., and Hannon, G.J. (2007). MIWI2 Is essential for spermatogenesis and repression of transposons in the mouse male germline. Dev. Cell *12*, 503–514.
14. Aravin, A., Gaidatzis, D., Pfeffer, S., Lagos-Quintana, M., Landgraf, P., Iovino, N., Morris, P., Brownstein, M.J., Kuramochi-Miyagawa, S., Nakano, T., et al. (2006). A novel class of small RNAs bind to MILI protein in mouse testes. Nature *442*, 203–207.
15. Gou, L.-T., Dai, P., Yang, J.-H., Xue, Y., Hu, Y.-P., Zhou, Y., Kang, J.-Y., Wang, X., Li, H., Hua, M.-M., et al. (2014). Pachytene piRNAs instruct massive mRNA elimination during late spermiogenesis. Cell Res. *24*, 680–700.
16. Castañeda, J., Genzor, P., van der Heijden, G.W., Sarkeshik, A., Yates, J.R., Ingolia, N.T., and Bortvin, A. (2014). Reduced pachytene piRNAs and translation underlie spermiogenic arrest in Maelstrom mutant mice. EMBO J *33*, 1999–2019.
17. Goh, W.S.S., Falciatori, I., Tam, O.H., Burgess, R., Meikar, O., Kotaja, N., Hammell, M., and Hannon, G.J. (2015). piRNA-directed cleavage of meiotic transcripts regulates spermatogenesis. Genes Dev. *29*, 1032–1044.
18. Czech, B., Munafò, M., Ciabrelli, F., Eastwood, E.L., Fabry, M.H., Kneuss, E., and Hannon, G.J. (2018). piRNA-guided genome defense: from biogenesis to silencing. Annu. Rev. Genet. *52*, 131–157.
19. Beyret, E., Liu, N., and Lin, H. (2012). piRNA biogenesis during adult spermatogenesis in mice is independent of the ping-pong mechanism. Cell Res. *22*, 1429–1439.
20. Lehtiniemi, T., and Kotaja, N. (2018). Germ granule-mediated RNA regulation in male germ cells. Reproduction *155*, R77–R91.
21. Tan, Y.-Q., Tu, C., Meng, L., Yuan, S., Sjaarda, C., Luo, A., Du, J., Li, W., Gong, F., Zhong, C., et al. (2019). Loss-of-function mutations in TDRD7 lead to a rare novel syndrome combining congenital cataract and nonobstructive azoospermia in humans. Genet. Med. *21*, 1209–1217.
22. Arafat, M., Har-Vardi, I., Harlev, A., Levitas, E., Zeadna, A., Abofoul-Azab, M., Dyomin, V., Sheffield, V.C., Lunenfeld, E., Huleihel, M., and Parvari, R. (2017). Mutation in TDRD9 causes non-obstructive azoospermia in infertile men. J. Med. Genet. *54*, 633–639.
23. Li, L., Tan, Y.Q., and Lu, L.Y. (2022). Defective piRNA processing and azoospermia. N. Engl. J. Med. *386*, 1675–1676.
24. Xiol, J., Cora, E., Koglgruber, R., Chuma, S., Subramanian, S., Hosokawa, M., Reuter, M., Yang, Z., Berninger, P., Palencia, A., et al. (2012). A role for Fkbp6 and the chaperone machinery in piRNA amplification and transposon silencing. Mol. Cell *47*, 970–979.

25. Preall, J.B., Czech, B., Guzzardo, P.M., Muerdter, F., and Hannon, G.J. (2012). shutdown is a component of the Drosophila piRNA biogenesis machinery. RNA *18*, 1446–1457.
26. Bonner, J.M., and Boulianne, G.L. (2017). Diverse structures, functions and uses of FK506 binding proteins. Cell. Signal. *38*, 97–105.
27. Lamb, J.R., Tugendreich, S., and Hieter, P. (1995). Tetratrico peptide repeat interactions: to TPR or not to TPR? Trends Biochem. Sci. *20*, 257–259.
28. Ichiyanagi, T., Ichiyanagi, K., Ogawa, A., Kuramochi-Miyagawa, S., Nakano, T., Chuma, S., Sasaki, H., and Udono, H. (2014). HSP90α plays an important role in piRNA biogenesis and retrotransposon repression in mouse. Nucleic Acids Res. *42*, 11903–11911.
29. Vagin, V.V., Wohlschlegel, J., Qu, J., Jonsson, Z., Huang, X., Chuma, S., Girard, A., Sachidanandam, R., Hannon, G.J., and Aravin, A.A. (2009). Proteomic analysis of murine Piwi proteins reveals a role for arginine methylation in specifying interaction with Tudor family members. Genes Dev. *23*, 1749–1762.
30. Zoch, A., Auchynnikava, T., Berrens, R.V., Kabayama, Y., Schöpp, T., Heep, M., Vasiliauskaitė, L., Pérez-Rico, Y.A., Cook, A.G., Shkumatava, A., et al. (2020). SPOCD1 is an essential executor of piRNA-directed de novo DNA methylation. Nature *584*, 635–639.
31. Crackower, M.A., Kolas, N.K., Noguchi, J., Sarao, R., Kikuchi, K., Kaneko, H., Kobayashi, E., Kawai, Y., Kozieradzki, I., Landers, R., et al. (2003). Essential Role of Fkbp6 in male fertility and homologous chromosome pairing in meiosis. Science *300*, 1291–1295.
32. Oud, M.S., Smits, R.M., Smith, H.E., Mastrorosa, F.K., Holt, G.S., Houston, B.J., de Vries, P.F., Alobaidi, B.K.S., Batty, L.E., Ismail, H., et al. (2022). A de novo paradigm for male infertility. Nat. Commun. *13*, 154.
33. Stokowy, T., Garbulowski, M., Fiskerstrand, T., Holdhus, R., Labun, K., Sztromwasser, P., Gilissen, C., Hoischen, A., Houge, G., Petersen, K., et al. (2016). RareVariantVis: new tool for visualization of causative variants in rare monogenic disorders using whole genome sequencing data. Bioinformatics *32*, 3018–3020.
34. Karczewski, K.J., Francioli, L.C., Tiao, G., Cummings, B.B., Alföldi, J., Wang, Q., Collins, R.L., Laricchia, K.M., Ganna, A., Birnbaum, D.P., et al. (2020). The mutational constraint spectrum quantified from variation in 141, 456 humans. Nature *581*, 434–443.
35. Robinson, J.T., Thorvaldsdóttir, H., Winckler, W., Guttman, M., Lander, E.S., Getz, G., and Mesirov, J.P. (2011). Integrative genomics viewer. Nat. Biotechnol. *29*, 24–26.
36. Richards, S., Aziz, N., Bale, S., Bick, D., Das, S., Gastier-Foster, J., Grody, W.W., Hegde, M., Lyon, E., Spector, E., et al. (2015). Standards and guidelines for the interpretation of sequence variants: a joint consensus recommendation of the American College of Medical Genetics and Genomics and the Association for Molecular Pathology. Genet. Med. *17*, 405–424.
37. Wyrwoll, M.J., Temel, Ş.G., Nagirnaja, L., Oud, M.S., Lopes, A.M., van der Heijden, G.W., Heald, J.S., Rotte, N., Wistuba, J., Wöste, M., et al. (2020). Bi-allelic mutations in M1AP are a frequent cause of meiotic arrest and severely impaired spermatogenesis leading to male infertility. Am. J. Hum. Genet. *107*, 342–351.
38. Wyrwoll, M.J., van Walree, E.S., Hamer, G., Rotte, N., Motazacker, M.M., Meijers-Heijboer, H., Alders, M., Meißner, A., Kaminsky, E., Wöste, M., et al. (2021). Bi-allelic variants in DNA mismatch repair proteins MutS Homolog MSH4 and MSH5 cause infertility in both sexes. Hum. Reprod. *37*, 178–189.
39. Salas-Huetos, A., Tüttelmann, F., Wyrwoll, M.J., Kliesch, S., Lopes, A.M., Goncalves, J., Boyden, S.E., Wöste, M., Hotaling, J.M., GEMINI Consortium, et al. (2021). Disruption of human meiotic telomere complex genes TERB1, TERB2 and MAJIN in men with non-obstructive azoospermia. Hum. Genet. *140*, 217–227.
40. Hardy, J.J., Wyrwoll, M.J., Mcfadden, W., Malcher, A., Rotte, N., Pollock, N.C., Munyoki, S., Veroli, M.V., Houston, B.J., Xavier, M.J., et al. (2021). Variants in GCNA, X-linked germ-cell genome integrity gene, identified in men with primary spermatogenic failure. Hum. Genet. *140*, 1169–1182.
41. Krausz, C., Riera-Escamilla, A., Moreno-Mendoza, D., Holleman, K., Cioppi, F., Algaba, F., Pybus, M., Friedrich, C., Wyrwoll, M.J., Casamonti, E., et al. (2020). Genetic dissection of spermatogenic arrest through exome analysis: clinical implications for the management of azoospermic men. Genet. Med. *22*, 1956–1966.
42. Riera-Escamilla, A., Vockel, M., Nagirnaja, L., Xavier, M.J., Carbonell, A., Moreno-Mendoza, D., Pybus, M., Farnetani, G., Rosta, V., Cioppi, F., et al. (2022). Large-scale analyses of the X chromosome in 2, 354 infertile men discover recurrently affected genes associated with spermatogenic failure. Am. J. Hum. Genet. *109*, 1458–1471.
43. Pedersen, B.S., Bhetariya, P.J., Brown, J., Kravitz, S.N., Marth, G., Jensen, R.L., Bronner, M.P., Underhill, H.R., and Quinlan, A.R. (2020). Somalier: rapid relatedness estimation for cancer and germline studies using efficient genome sketches. Genome Med. *12*, 62.
44. Abou Tayoun, A.N., Pesaran, T., DiStefano, M.T., Oza, A., Rehm, H.L., Biesecker, L.G., Harrison, S.M.; and ClinGen Sequence Variant Interpretation Working Group ClinGen SVI (2018). Recommendations for interpreting the loss of function PVS1 ACMG/AMP variant criterion. Hum. Mutat. *39*, 1517–1524.
45. Harrison, S.M., Biesecker, L.G., and Rehm, H.L. (2019). Overview of specifications to the ACMG/AMP variant interpretation guidelines. Curr. Protoc. Hum. Genet. *103*, e93.
46. Rehm, H.L., Berg, J.S., Brooks, L.D., Bustamante, C.D., Evans, J.P., Landrum, M.J., Ledbetter, D.H., Maglott, D.R., Martin, C.L., Nussbaum, R.L., et al. (2015). ClinGen — The Clinical Genome Resource. N. Engl. J. Med. *372*, 2235–2242.
47. Kechin, A., Boyarskikh, U., Kel, A., and Filipenko, M. (2017). cutPrimers: a new tool for accurate cutting of primers from reads of targeted next generation sequencing. J. Comput. Biol. *24*, 1138–1143.
48. Langmead, B., Trapnell, C., Pop, M., and Salzberg, S.L. (2009). Ultrafast and memory-efficient alignment of short DNA sequences to the human genome. Genome Biol. *10*, R25.
49. Kuksa, P.P., Amlie-Wolf, A., Katanić, Ž., Valladares, O., Wang, L.-S., and Leung, Y.Y. (2019). DASHR 2.0: integrated database of human small non-coding RNA genes and mature products. Bioinformatics *35*, 1033–1039.
50. Girard, A., Sachidanandam, R., Hannon, G.J., and Carmell, M.A. (2006). A germline-specific class of small RNAs binds mammalian Piwi proteins. Nature *442*, 199–202.

51. Andy Bunn, M.K. (2017). A language and environment for statistical computing. R Found. Stat. Comput. *10*, 11–18.
52. Virtanen, P., Gommers, R., Oliphant, T.E., Haberland, M., Reddy, T., Cournapeau, D., Burovski, E., Peterson, P., Weckesser, W., Bright, J., et al. (2020). SciPy 1.0: fundamental algorithms for scientific computing in Python. Nat. Methods *17*, 261–272.
53. Mescheriakova, J.Y., Verkerk, A.J., Amin, N., Uitterlinden, A.G., van Duijn, C.M., and Hintzen, R.Q. (2019). Linkage analysis and whole exome sequencing identify a novel candidate gene in a Dutch multiple sclerosis family. Mult. Scler. *25*, 909–917.
54. Vilariño-Güell, C., Encarnacion, M., Bernales, C.Q., and Sadovnick, A.D. (2019). Analysis of Canadian multiple sclerosis patients does not support a role for FKBP6 in disease. Mult. Scler. *25*, 1011–1013.
55. Gomes Fernandes, M., He, N., Wang, F., Van Iperen, L., Eguizabal, C., Matorras, R., Roelen, B.A.J., and Chuva De Sousa Lopes, S.M. (2018). Human-specific subcellular compartmentalization of P-element induced wimpy testis-like (PIWIL) granules during germ cell development and spermatogenesis. Hum. Reprod. *33*, 258–269.
56. Özata, D.M., Yu, T., Mou, H., Gainetdinov, I., Colpan, C., Cecchini, K., Kaymaz, Y., Wu, P.-H., Fan, K., Kucukural, A., et al. (2020). Evolutionarily conserved pachytene piRNA loci are highly divergent among modern humans. Nat. Ecol. Evol. *4*, 156–168.
57. Wang, M., Liu, X., Chang, G., Chen, Y., An, G., Yan, L., Gao, S., Xu, Y., Cui, Y., Dong, J., et al. (2018). Single-Cell RNA sequencing analysis reveals sequential cell fate transition during human spermatogenesis. Cell Stem Cell *23*, 599–614.e4.
58. Guo, J., Grow, E.J., Mlcochova, H., Maher, G.J., Lindskog, C., Nie, X., Guo, Y., Takei, Y., Yun, J., Cai, L., et al. (2018). The adult human testis transcriptional cell atlas. Cell Res. *28*, 1141–1157.
59. Sciurano, R.B., Rahn, M.I., Rey-Valzacchi, G., Coco, R., and Solari, A.J. (2012). The role of asynapsis in human spermatocyte failure. Int. J. Androl. *35*, 541–549.
60. Nakata, H., Wakayama, T., Asano, T., Nishiuchi, T., and Iseki, S. (2017). Identification of sperm equatorial segment protein 1 in the acrosome as the primary binding target of peanut agglutinin (PNA) in the mouse testis. Histochem. Cell Biol. *147*, 27–38.
61. Yang, F., and Wang, P.J. (2016). Multiple LINEs of retrotransposon silencing mechanisms in the mammalian germline. Semin. Cell Dev. Biol. *59*, 118–125.
62. Macia, A., Widmann, T.J., Heras, S.R., Ayllon, V., Sanchez, L., Benkaddour-Boumzaouad, M., Muñoz-Lopez, M., Rubio, A., Amador-Cubero, S., Blanco-Jimenez, E., et al. (2017). Engineered LINE-1 retrotransposition in nondividing human neurons. Genome Res. *27*, 335–348.
63. Wyrwoll, M.J., Köckerling, N., Vockel, M., Dicke, A.-K., Rotte, N., Pohl, E., Emich, J., Wöste, M., Ruckert, C., Wabschke, R., et al. (2022). Genetic architecture of azoospermia—time to advance the standard of care. Eur. Urol. https://doi.org/10.1016/j.eururo.2022.05.011.
64. Hsieh, C.L., Xia, J., and Lin, H. (2020). MIWI prevents aneuploidy during meiosis by cleaving excess satellite RNA. EMBO J *39*, e103614.
65. Reuter, M., Chuma, S., Tanaka, T., Franz, T., Stark, A., and Pillai, R.S. (2009). Loss of the mili-interacting tudor domain-containing protein-1 activates transposons and alters the Mili-associated small RNA profile. Nat. Struct. Mol. Biol. *16*, 639–646.
66. Deng, W., and Lin, H. (2002). miwi, a murine homolog of piwi, encodes a cytoplasmic protein essential for spermatogenesis. Dev. Cell *2*, 819–830.
67. Ding, D., Liu, J., Dong, K., Midic, U., Hess, R.A., Xie, H., Demireva, E.Y., and Chen, C. (2017). PNLDC1 is essential for piRNA 3′ end trimming and transposon silencing during spermatogenesis in mice. Nat. Commun. *8*, 819.
68. Zheng, K., and Wang, P.J. (2012). Blockade of pachytene piRNA biogenesis reveals a novel requirement for maintaining post-meiotic germline genome integrity. PLoS Genet. *8*, e1003038.